3D SHALLOW WATER ACOUSTICS

Ying-Tsong Lin Woods Hole Oceanographic Institution, Woods Hole, MA, USA

1 INTRODUCTION

Both marine geological features and physical oceanographic processes in continental shelves and shelfbreak areas can cause horizontal heterogeneity in medium properties, so horizontal reflection/ refraction of sound can occur and produce significant three-dimensional (3-D) sound propagation effects. The long-term goals of this research are focused on investigation of the 3-D acoustic effects and their temporal and spatial variability caused by the environmental factors commonly observed, such as bathymetric slopes, submarine canyons, surface waves, internal waves and shelfbreak fronts. Figure 1 depicts the environmental variability considered in this study: (1) water column sound speed fluctuations caused by internal waves (shown), shelfbreak fronts, and sub-mesoscale eddies, (2) submarine canyons, (3) shelfbreak and slopes, (4) 3-D sub-bottom with interface irregularity and roughness, and (5) surface waves.

In a recent meeting of the Acoustical Society of America (the 2015 Pittsburg meeting), a series of invited papers was presented in an underwater acoustics special session for 3-D sound propagation and scattering studies. These papers covered topics from numerical methods [1-5], laboratorial experiments [6-8], and field work experiment [1,9]. Reported in this paper, the research objectives include development of efficient and accurate 3-D sound propagation model for complex ocean environments. The ultimate goal of this research is to study the underlying physics of the 3-D sound propagation effects produced jointly by physical oceanographic processes and geological features. To achieve that, individual environmental factor are first studied and then considered jointly with a unified ocean, seabed and acoustic model. Another major objective is to develop a sound pressure sensitivity analysis method to predict acoustic fluctuations and assess the joint ocean and seabed effects.

2 METHODS

The technical approaches employed in this 3D sound propagation study include theoretical analysis, numerical computation and real data analysis. A 3-D normal mode method has been used to study canonical environmental models of shelfbreak front systems [11] and nonlinear internal wave ducts [12-13]. 3-D parabolic-equation (PE) wave propagation models with improved split-step marching algorithms [14-16] are used to study sound propagation in realistic environments. When the acoustic mode coupling can be neglected, a vertical-mode horizontal-PE model can be used. In this section, the numerical methods utilizing the PE approximation will be briefly reviewed.

The PE approximation method, first introduced by Tappert [17] to underwater acoustic modeling, has long been recognized as one of the most efficient and effective numerical methods to predict sound propagation in complex environments. The advantage of this method is due to the fact that it converts the Helmholtz wave equation of elliptic type to a one-way wave equation of parabolic type. This enables efficient marching solution algorithms (see Figure 2) for solving the boundary value problem posed by the Helmholtz equation. This can greatly reduce the computational resources for modeling 3-D sound propagation.

Another numerical method to predict acoustic fluctuations due to 3-D sound speed perturbation in the water column is a tangent linear PE model. The details of this method are referred to Ref. [18], and it is briefed here along with an application to determine the sound pressure sensitivity kernel with respect to changes in the index of refraction of the medium.

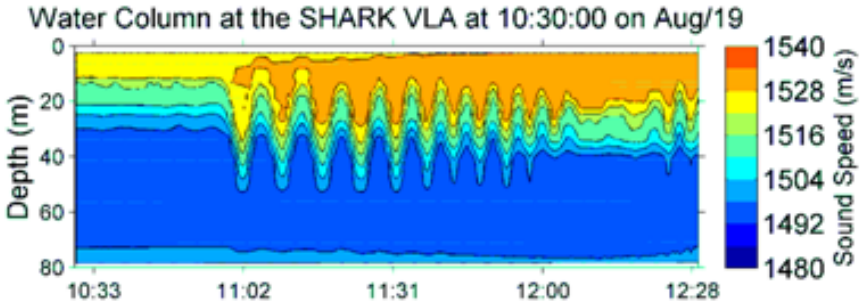

(a) Water-column sound speed perturbations by internal gravity waves

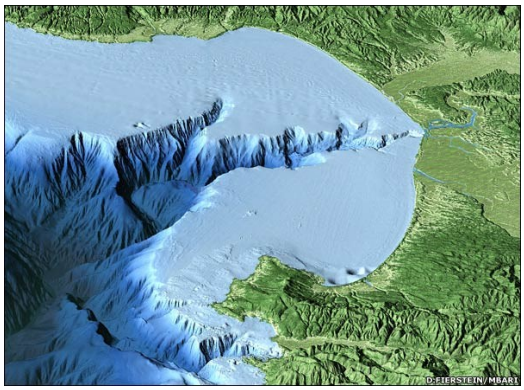

(b) Submarine Canyons
Monterey Canyon
© Monterey Bay Aquarium Research Institute

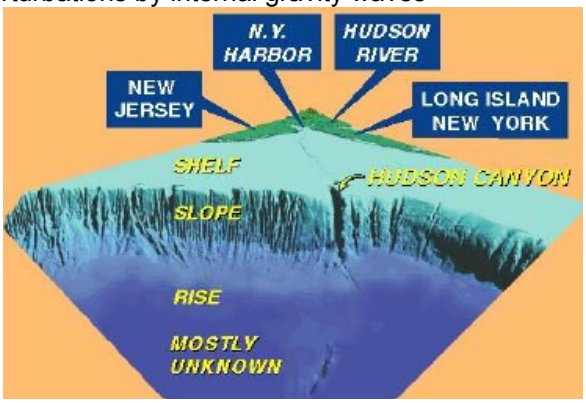

(c) Shelfbreak and slope
NJ shelf and Hudson canyon area
Image courtesy of Hudson Canyon 2002, NOAA/OER

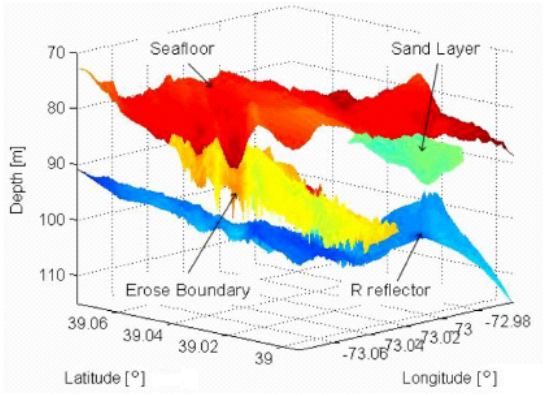

(d) 3-D sub-bottom structure
Rough seafloor and sub-bottom interfaces on NJ Shelf
Ballard, Becker and Goff, IEEE JOE, 2010 [10]

(e) Surface water waves
Artwork by Kerem Gogus

Figure 1: The types of environments considered in this research study. Due to the present of strong horizontal gradients in seafloor topography, sub-bottom layering and the index of refraction, these marine geological and physical oceanographic features can produce strong 3-D sound propagation effects.

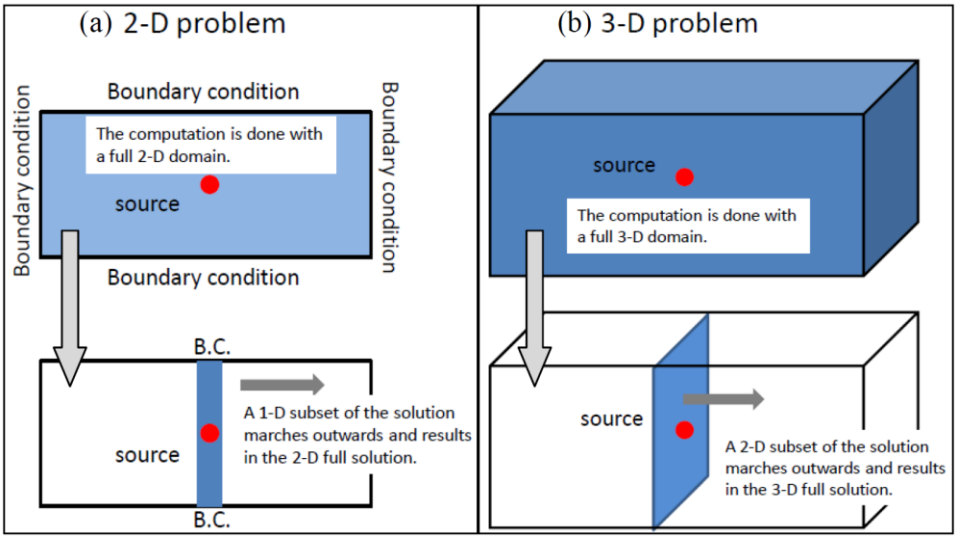

Figure 2. Dimension reduction of the Helmholtz equation by the parabolic-equation approximation.

Consider the following one-way parabolic wave equation,

$$\frac{\partial}{\partial x}u(x,y,z) = ik_{\text{ref}}\left\{-1+\sqrt{k_{\text{ref}}^{-2}\nabla_{\perp}^{2}+n^{2}(x,y,z)}\right\}u(x,y,z), \tag{1}$$

where u is the demodulated sound pressure with the baseline phase removed according to the reference wavenumber k_{ref}, i.e., $u = p\exp(-ik_{\text{ref}}x)$, and n is the index of refraction with respect to k_{ref}. Note that the exact PE operator consisting of the square-root Helmholtz operator is

$$\mathcal{L} = -1+\sqrt{k_{\text{ref}}^{-2}\nabla_{\perp}^{2}+n^{2}(x,y,z)}. \tag{2}$$

Now, let $n^2(x,y,z) = \gamma_0(x,y,z) + \varepsilon\gamma_1(x,y,z)$, where γ_0 is the square of the index of refraction of the background state, and γ_1 is a perturbation scaled by an arbitrary small parameter ε. The background PE operator is

$$\mathcal{L}_0 = -1+\sqrt{k_{\text{ref}}^{-2}\nabla_{\perp}^{2}+\gamma_0(x,y,z)}, \tag{3}$$

and there are various approximations made for $\mathcal{L}$ with respect to the perturbation of the index of refraction γ_1. Hursky et al. [19] and Smith [20] have showed the tangent linear operators for the standard narrow-angle and wide-angle PE's. In this project, the higher-order operator splitting algorithm (1) is used to derive a higher-order tangent linear operator that unifying previous formula:

$$\mathcal{L}_3 = \mathcal{L}_0 + \frac{1}{2}\left[(1-\mathcal{L}_0)\left(-1+\sqrt{1+\varepsilon\gamma_1}\right)+\left(-1+\sqrt{1+\varepsilon\gamma_1}\right)(1-\mathcal{L}_0)\right]. \tag{4}$$

The corresponding higher-order tangent linear PE solution with $\mathcal{L}_3$ is:

$$u(x+\Delta x,y,z) \cong e^{ik_{\text{ref}}\Delta x\mathcal{L}_0}\left[1+\frac{ik_{\text{ref}}}{2}\Delta x(1-\mathcal{L}_0)\varepsilon\gamma_1\right]u(x,y,z), \tag{5}$$

where $\mathcal{L}_0$ and γ_1 are assumed to be commutative.

From the higher-order tangent linear PE solution (5), we can deduce the following local tangent kernel to determine the gradient of the sound pressure with respect to n^2 at a given position $\vec{x}'$.

$$\frac{\partial(p|_{\vec{x}'})}{\partial(n^2|_{\vec{x}'})} = \frac{ik_{\mathrm{ref}}}{2}\,(1-\mathcal{L}_0)\,p(\vec{x}') \tag{6}$$

By incorporating the Green's function between the perturbation position $\vec{x}'$ and the receiver position $\vec{x}$, one can obtain the following sensitivity kernel:

$$\frac{\partial(p|_{\vec{x}})}{\partial(n^2|_{\vec{x}'})} = G(\vec{x};\vec{x}')\frac{\partial(p|_{\vec{x}'})}{\partial(n^2|_{\vec{x}'})}. \tag{7}$$

Another new algorithm to make the boundaries of the 3-D PE model grid fit right on to irregular or rough surface has been developed. This method utilizes the ADI Split-Step Padé algorithm [16] and the 1-D Galerkin discretization with variable grid sizes [21] on each ADI step (see Figure 3). This algorithm has tested and benchmarked with a semi-circular waveguide problem. The numerical performance is verified, and the algorithm can be utilized for computing 3-D forward scattering from rough sea surface and bottom interfaces. A future research plan to develop a two-way 3-D PE algorithm is proposed to provide numerical solutions of forward and backward scattering field.

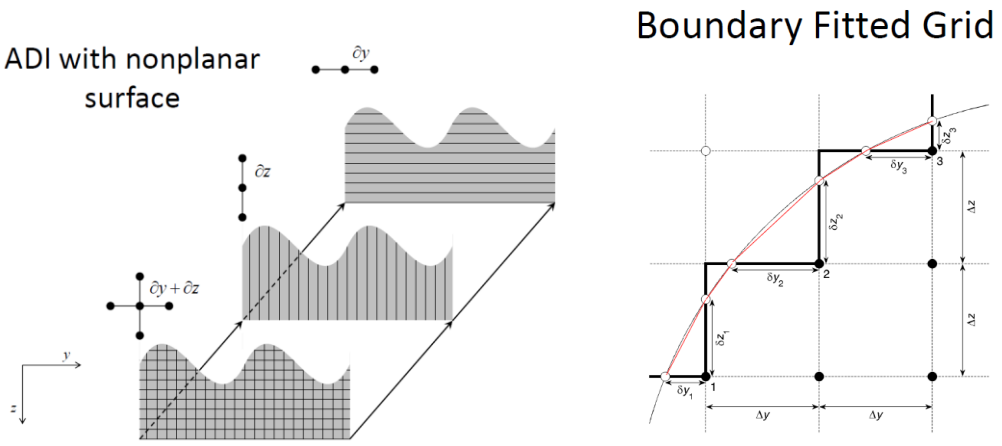

Figure 3. Illustration of the boundary-fitted 3-D PE algorithm for handling nonplanar (irregular or rough) sea surface.

3 RESULTS

Some examples of study results are presented in this section.

3.1 3-D sound propagation effects caused by topographical variability

Besides numerical simulations of sound propagation in canyons and seamounts (examples are shown in Figures 4 and 5), the sound propagation effects caused by submarine canyons have also been studied using the transmission loss (TL) data collected during an sea-going experiment sponsored jointly by the Office of Naval Research, USA and the National Science Council, Taiwan [22], where mobile acoustic sources were utilized to study sound propagation over North Mein-Hua Canyon. A 3-D PE model [14] was employed to investigate the underlying physics. The acoustic data show a significant decrease in sound intensity as the source crossed over the canyon, and the numerical model produces comparable results due to this shadowing effect. In addition, the model suggests that 3-D sound focusing due to the canyon seafloor can occur when the underwater sound

propagates along the canyon axis. A preliminary study has been performed to examine the effects of bathymetric and bottom property uncertainties. Between these two uncertainties, it was found that the bathymetry affects sound field complexity more over a submarine canyon, because bathymetric errors can transfer into TL errors through incorrect bottom interaction [22].

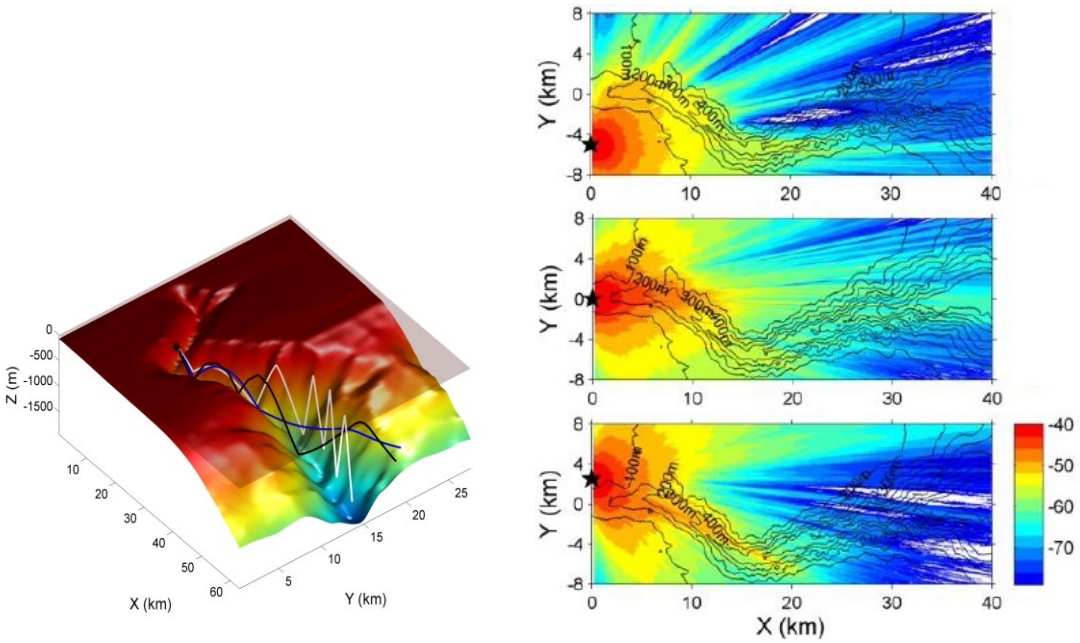

Figure 4. Realistic Hudson canyon model. The left panel shows the canyon bathymetry, and the right panels shows the numerical solutions of sound pressure fields due to three different source poisitions. Effects of sound focusing and cutoff can be observed.

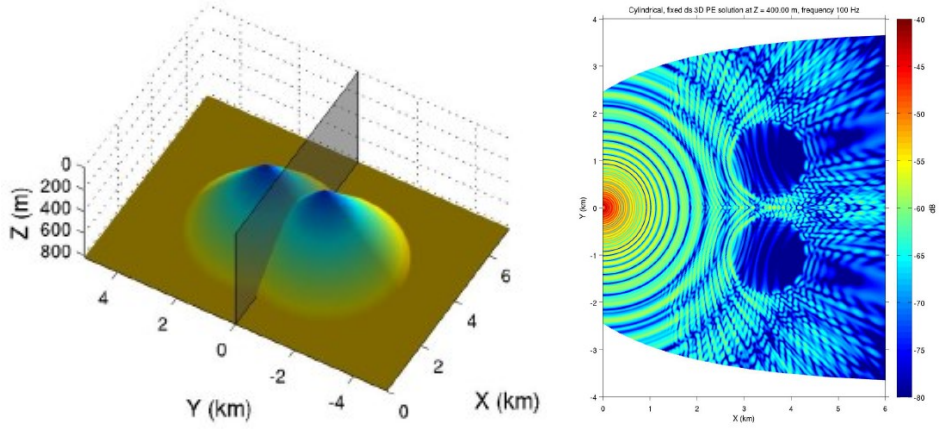

Figure 5. PE solution of underwater sound propagation through a double seamount.

3.2 3-D sound propagation effects caused by gravity waves

The first experimental observation of low-frequency horizontal acoustic ducting between nonlinear internal gravity waves was made by Badiey et al. [23]. More evidence of acoustic ducting, sound radiation from the end of internal wave ducts, and fluctuations in the horizontal angle of arrival were observed in the Shallow Water 2006 Experiment [24-25]. Numerical raytracing of sound in a curved nonlinear internal gravity wave duct is shown in Figure 6. It is observed that sound can be ducted

between internal waves of depression. In Figure 6, three rays emitted with the same azimuth but different vertical angles have different propagation paths. The ray with the shallowest angle goes underneath the waves and passes though them. As the vertical angle increases, the ray starts to be trapped in between waves. Initially along the outer wave, when the angle becomes steeper, the ray will bounce between the two waves. This propagation behavior can also be seen in a 3-D mode analysis [26]; in brief, the ray path along the outer wave will form horizontal whispering gallery modes, and the ray bouncing between waves will from fully bouncing modes.

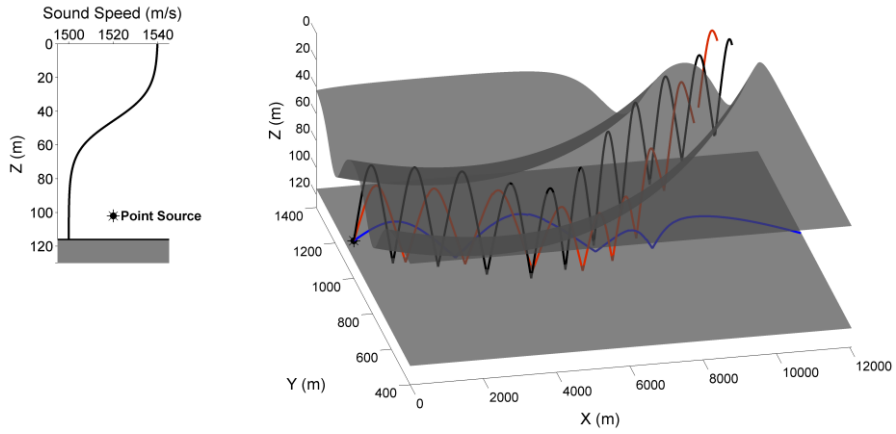

Figure 6. 3-D Raytracing of sound in a curved internal wave duct.

The second example is sound propagation in a waveguide with non-planar surface as shown in Figure 7. The depth of the waveguide is 195 m, and the amplitude and wavelength of the idealized surface waves is 5 m and 1 km, respectively. A 25-Hz point source is placed 100 m below a surface wave crest, and the ADI Padé PE method with the boundary-fitted grid is utilized to compute the sound pressure field. The TL solution at 30 m depth is shown, and the horizontal focusing along the surface wave crest that the source is placed below. A benchmark problem with a semi-circular waveguide is developed to check the PE solutions.

3.3 Sound pressure field sensitivity analysis

A tangent linear 3D PE solution to predict acoustic variations due to sound speed perturbation has been developed [18]. With this tangent linear solution, we can derive a sound pressure sensitivity kernel, as shown in the previous section. An example of sound pressure sensitivity analysis in an internal wave acoustic duct is shown in Figure 8. The internal wave displacement is shown in the panel (a), where one can see that the source is placed underneath the first wave crest. The sensitivity kernel of sound pressure square with respect to sound speed between the source and a receiver underneath the second wave crest is shown in the panel (b), and lastly, the sound pressure sensitivity and its dynamics following the internal wave motion is in (c). The sensitivity kernel has been converted to be per wave height through a chain rule.

4 SUMMARY

This paper briefly reviews studies of 3-D sound propagation in areas of continental shelf and shelfbreak due to a variety of marine geological and physical oceanographic features. The main contributions of the research are on assessing the environment-induced acoustic impacts and on increasing the capability of sonar systems in complex shallow water areas.

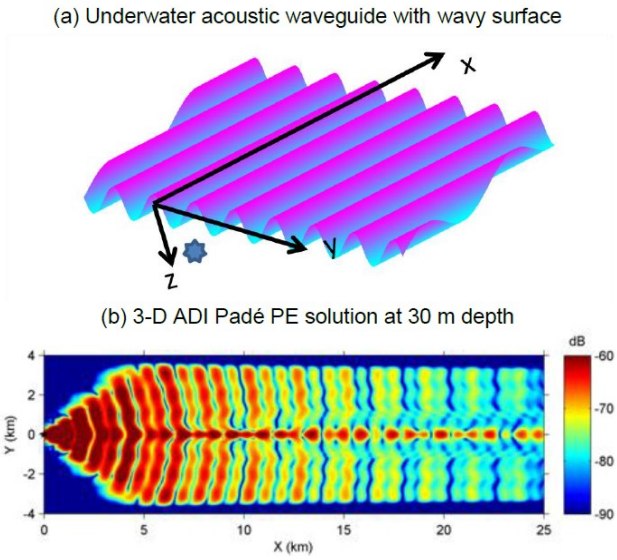

Figure 7. ADI Padé PE solution of 3-D sound propagation in an idealized underwater waveguide with wavy surface. Note that numerical sponge layers are placed on the sides of the domain to mimic a radiation boundary condition.

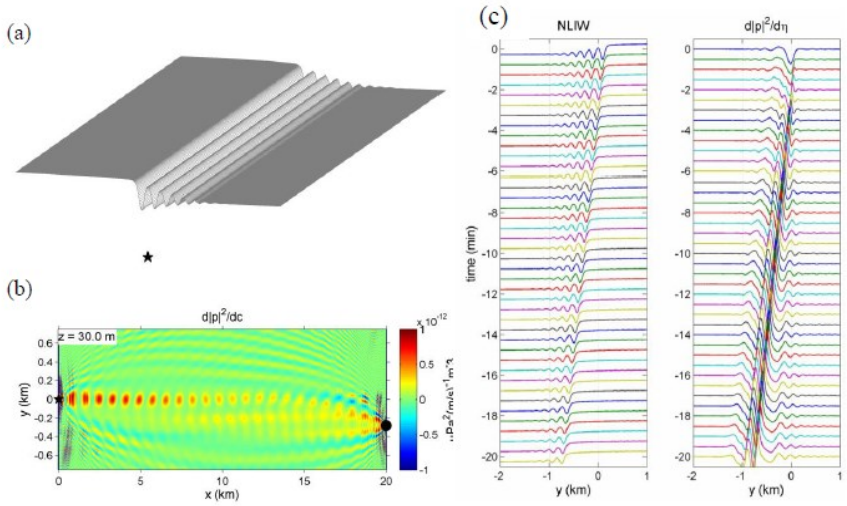

Figure 8. Sensitivity analysis an internal wave acoustic duct.

5 REFERENCES

1. K.D. Heaney and R.L. Campbell, 'Three-dimensional propagation in the open ocean: Observations and modeling (A)', J. Acoust. Soc. Am., vol. 137, p.2389 (2015).
2. M.B. Porter, 'Out-of-plane effects in three-dimensional oceans (A)', J. Acoust. Soc. Am., vol. 137, p.2419 (2015).
3. A.T. Abawi, 'Numerically exact three-dimensional propagation (A)', J. Acoust. Soc. Am., vol. 137, p.2419 (2015).
4. M.S. Ballard, 'Coupled mode analysis of three-dimensional propagation over a cosine shaped hill (A)', J. Acoust. Soc. Am., vol. 137, p.2419 (2015).

5. T.F. Duda, A.E. Newhall and Y.-T. Lin, 'Links between acoustic field statistics, baroclinic wave geometry, and bathymetry computed with time-stepped three-dimensional acoustic simulations (A)', J. Acoust. Soc. Am., vol. 137, p.2420 (2015).
6. F. Sturm, J.-P. Sessarego, and Alexios Korakas, 'Laboratory scale measurements of three-dimensional sound propagation in the presence of a tilted penetrable bottom (A)', J. Acoust. Soc. Am., vol. 137, p.2390 (2015).
7. J. Sagers, 'Measurements of three-dimensional acoustic propagation in a scale-model canyon (A)', J. Acoust. Soc. Am., vol. 137, p.2391 (2015).
8. L. Zhang, H.L. Swinney, and Y.-T. Lin, 'Laboratory measurements of sound propagation in a continuously stratified ocean containing internal waves (A)', J. Acoust. Soc. Am., vol. 137, p.2390 (2015).
9. M. Badiey, 'The role of water column variability on three-dimensional sound propagation in shallow water (A)', J. Acoust. Soc. Am., vol. 137, p.2389 (2015).
10. M.S. Ballard, K.M. Becker, and J.A. Goff, 'Geoacoustic Inversion for the New Jersey Shelf: 3-D Sediment Model'; IEEE J. Oceanic Eng., 35, 28-42. (2010).
11 Y.-T. Lin and J.F. Lynch, 'Analytical study of the horizontal ducting of sound by an oceanic front over a slope, ' J. Acoust. Soc. Am., vol. 131, pp. EL1-EL7 (2012).
12 Y.-T Lin, T.F. Duda and J.F. Lynch, 'Acoustic mode radiation from the termination of a truncated nonlinear internal gravity wave duct in a shallow ocean area', J. Acoust. Soc. Am., vol. 126, pp. 1752-1765 (2009).
13 Y.-T. Lin, K.G. McMahon, J.F. Lynch, and W.L. Siegmann, 'Horizontal ducting of sound by curved nonlinear internal gravity waves in the continental shelf areas,' J. Acoust. Soc. Am., vol. 133, pp. 37-49 (2013).
14 Y.-T. Lin, T.F. Duda, and A.E. Newhall, 'Three-dimensional sound propagation models using the parabolic-equation approximation and the split-step Fourier method,' J. Comp. Acoust., vol. 21, 1250018 (2013).
15 Y.-T. Lin and T.F. Duda, 'A higher-order split-step Fourier parabolic-equation sound propagation solution scheme,' J. Acoust. Soc. Am, vol. 132, pp. EL61-EL67 (2012).
16 Y.-T. Lin, J.M. Collis and T.F. Duda, 'A three-dimensional parabolic equation model of sound propagation using higher-order operator splitting and Padé approximants,' J. Acoust. Soc. Am., vol. 132, pp. EL364-370 (2012).
17 F. D. Tappert, Parabolic equation method in underwater acoustics, J. Acoust. Soc. Am., vol. 55, p. S34 (1974).
18 Y.-T. Lin, 'A higher-order tangent linear parabolic-equation solution of three-dimensional sound propagation, ' J. Acoust. Soc. Am., vol. 134, pp. EL251-EL257 (2013).
19 P. Hursk, M. B. Porter, B. D. Cornuelle, W. S. Hodgkiss, and W. A. Kuperman, 'Adjoint modeling for acoustic inversion,' J. Acoust. Soc. Am., vol. 115, 607–619 (2004)
20 K. B. Smith, 'Adjoint modeling with a split-step Fourier parabolic equation model (L),' J. Acoust. Soc. Am., vol. 120, 1190–1191 (2006).
21 W.M. Sanders and M.D. Collins, 'Nonuniform depth grids in parabolic equation solutions', J. Acoust. Soc. Am., 133, 1953-1958 (2013).
22 Y.-T. Lin, T.F. Duda, C. Emerson, G.G. Gawarkiewicz, A.E. Newhall, B. Calder, J.F. Lynch, P. Abbot, Y.-J. Yang and S. Jan, 'Experimental and numerical studies of sound propagation over a submarine canyon northeast of Taiwan,' IEEE J. Ocean. Eng., 40, pp. 237-249 (2015).
23 M. Badiey, Y. Mu, J.F. Lynch, J.R. Apel, and S.N. Wolf, 'Temporal and azimuthal dependence of sound propagation in shallow water with internal waves,' IEEE J. Ocean. Eng. 27, 117-129 (2002).
24 Y.-T. Lin, T.F. Duda, and J.F. Lynch, 'Acoustic mode radiation from the termination of a truncated nonlinear internal gravity wave duct in a shallow ocean area,' J. Acoust. Soc. Am. 126, 1752-1765 (2009).
25 T.F. Duda, J.M. Collis, Y.-T. Lin, A.E. Newhall, J.F. Lynch, and H.A. DeFerrari, 'Horizontal coherence of low-frequency fixed-path sound in a continental shelf region with internal-wave activity,' J. Acoust. Soc. Am. 131, 1782-1797 (2012).
26 Y.-T. Lin, K.G. McMahon, J.F. Lynch, and W.L. Siegmann, 'Horizontal ducting of sound by curved nonlinear internal gravity waves in the continental shelf areas,' J. Acoust. Soc. Am. 133, 37-49 (2013).